

NEW FULLY ELECTROMAGNETIC SIMULATIONS OF SPRITES INITIATED BY RUNAWAY AIR BREAKDOWN

R.A. Roussel-Dupré⁽¹⁾, E.M.D. Symbalisy⁽²⁾, H.E. Tierney⁽³⁾, L. Triplett⁽⁴⁾

⁽¹⁾*PO Box 1663, EES-8, Mail Stop F665, Los Alamos National Laboratory, Los Alamos, New Mexico, USA, rroussel-dupre@lanl.gov*

⁽²⁾*As (1) above, but E-mail: esymbalisy@lanl.gov*

⁽³⁾*As (1) above, but E-mail: htierney@lanl.gov*

⁽⁴⁾*As (1) above, but E-mail: ltriplett@lanl.gov*

ABSTRACT

First principles, fully electromagnetic, 2-D simulations of high-altitude discharges that occur from cloud tops to approximately 90 km altitude were carried out. Both conventional and runaway air breakdown are included. The sprite simulation discussed in this paper is characterized by the formation of streamers that initiate at 70 km and propagate down to 55 km altitude followed by the development of a runaway discharge that propagates upward. At altitudes above 70 km conventional breakdown produces airglow over a large horizontal region with a diameter that can exceed 100 kilometers. Corresponding optical spectra, gamma ray emissions, and radio emissions are calculated.

INTRODUCTION

The existence of high-altitude optical transients that occur over the tops of thunderstorms is now well documented (see [1] for a review). Their association with high-altitude electrical discharges, first proposed by Wilson [2], seems no longer to be in question [3]. The only remaining issue is whether these events are glow discharges, 'streamers', breakdown caused by strong quasi-electrostatic fields, breakdown caused by strong electromagnetic pulses launched by cloud-to-ground or intracloud lightning, electrical breakdown of the air initiated by relativistic electrons (i.e. runaway air breakdown), or some combination of these various mechanisms. In this paper we extend our previous 2-D sprite simulations to a fully electromagnetic treatment that includes the important effects of induction and radiation. Both the runaway (as predicted by [4]) and conventional (as observed in the laboratory) breakdown mechanisms are included and evidence for the occurrence of both processes exists in the simulations as well as the observations.

The most direct observational evidence for the occurrence of runaway breakdown in association with high-altitude discharges arises from the measurements of the BATSE [5] experiment on the Compton Gamma Ray Observatory. This experiment measured bursts (several ms in duration) of energetic (10 keV to > 300 keV) photons that seemed to originate from thunderstorms. In order to escape the atmosphere these photons must have originated from altitudes above 25-30 km. Further evidence for the occurrence of the runaway mechanism in conjunction with other lightning discharge processes includes measurements taken from aircraft and balloons flying through thunderstorms and more recently from the ground in association with the leader activity that precedes the return stroke. One has the impression that runaway breakdown exists throughout the range of thunderstorm electrical discharges. There is the additional fact that the threshold for the runaway mechanism is a factor of ten less than that needed to initiate a conventional breakdown and that the macroscopic electric fields measured inside thunderstorms often exceed the runaway threshold but never reach that of conventional breakdown.

The evidence for conventional breakdown is rooted in comparisons between observations of natural lightning and the discharges that are induced in the laboratory. The smaller scales (mm) required for the development of a strong conventional discharge compared to the runaway scale-lengths (avalanche lengths exceeding tens of meters) makes it easier to develop streamers. The significantly smaller volumes and faster time scales thought to be associated with the conventional mechanism make it more likely to heat the air and produce blackbody radiation and to generate very high frequency (VHF) radiation in the radio bands of the electromagnetic spectrum. High spatial resolution observations of sprites above 60 km altitude reveal structures that are tens of meters in radial extent. These dimensions are more consistent with conventional breakdown. In addition, the threshold for conventional breakdown is more easily exceeded

at high-altitudes where the large scale lengths needed to drive runaway preclude its initiation there and prevent it from raising the electrical conductivity sufficiently to eliminate the electric field before reaching the conventional threshold.

We have noted only a few of the considerations that arise in distinguishing the runaway mechanism from conventional breakdown. Many details require further elaboration and will be left for a future, more extensive publication. We proceed with a discussion of our simulations and a presentation of preliminary results from one example.

SPRITE MODEL

We now describe an extension and modification of earlier work [6] that allows us to predict the full temporal evolution of lightning discharges. In the present analysis, we replace the quasi-electrostatic equations with the full set of Maxwell's equations. As a result we are now able to compute the induction and radiation fields (electric and magnetic fields) and include their effect on the electron and ion populations self-consistently. Our new formulation also allows for imposing a spatially divergent and temporally varying lightning current anywhere within the computational grid. This modification allows us to simulate the build-up of charge within a thunderstorm and to model high-altitude discharges. A momentum equation for the relativistic electrons has been added to our equation set. This added feature allows us to include the effect of magnetic pinching that is characteristic of high-current, relativistic electron beams. Our overall analysis can be described as follows.

Electromagnetic Equations

$$\frac{\partial \mathbf{B}}{\partial t} = -\nabla \times \mathbf{E}, \quad \frac{\partial \mathbf{D}}{\partial t} = \nabla \times \mathbf{H} - \mathbf{J}, \quad \mathbf{B} = \nabla \times \mathbf{H}, \quad \mathbf{D} = \epsilon \mathbf{E}, \quad \mathbf{J} = \nabla \times \mathbf{E} + \mathbf{J}_{Lightning} \quad (1)$$

The electric field in this formulation is the total field due to charge buildup from the lightning current density, due to charge buildup from the primary and secondary electron currents, and due to electromagnetic radiation. We use the vacuum values of ϵ_0 and μ_0 for air, and measured values for the ground. We deduce the air conductivity from the maximum of electron and ion currents, σ_{ei} (see below) and a measured altitude dependent ambient $\sigma_{ambient}$:

$$\sigma = \max(\sigma_{ambient}, \sigma_{ei})$$

$$\sigma_{ei} \mathbf{E} = e(n_s v_s + n_p v_p) \frac{\mathbf{E}}{|E|} + e(n_- + n_+) \mu_{ion} \mathbf{E} \quad (2)$$

Here, we have assumed that the electrons and negative ions are moving anti-parallel to the electric field and that the positive ions are moving parallel to E. We have also assumed that the ions are singly ionized and possess a mobility of:

$$\mu_{ion} \frac{m^2}{V s} = 2.27 \times 10^{14} \frac{\mu_0}{\sigma}, \quad \text{where } \mu_0 = 0.00123 \text{ gm/cc} \quad (3)$$

In our formulation we assume that the processes we are studying – lightning and lightning related discharges – can only increase the air conductivity. The ground electrical conductivity is set equal to a constant measured value.

Electron and Ion Continuity Equations and Primary Electron Momentum

We evolve in time the secondary and primary electron populations (n_s, n_p), and the positive and negative ion populations (n_+, n_-). We do not currently independently solve for the secondary electron momenta (or velocity) and energy. For the ions we use the previously listed mobility to find the ion velocities. For the secondary, or slow, electrons we compute their velocity (\mathbf{V}_s) from fits to swarm data. For the primary, or relativistic, electrons we compute the velocity (\mathbf{V}_p) from their energy taken from fits of Boltzmann equation solutions for the avalanche process. The source and sink terms for various particle species include R_p , the avalanche rate of runaway electrons, F_c , the flux of cosmic-ray produced high-energy electrons, $R_s = \frac{\epsilon_p}{\epsilon} R_p$, the production rate of secondary electrons by means of primary ionization, $\epsilon = 34 \text{ eV}$ is the energy loss per ion pair produced in air, α_i , the avalanche rate for low-energy electrons (ionization minus dissociative attachment), β , the three-body attachment rate, γ_r , the radiative recombination rate, and γ_{ii} , the ion-ion

recombination rate. Following [6]:

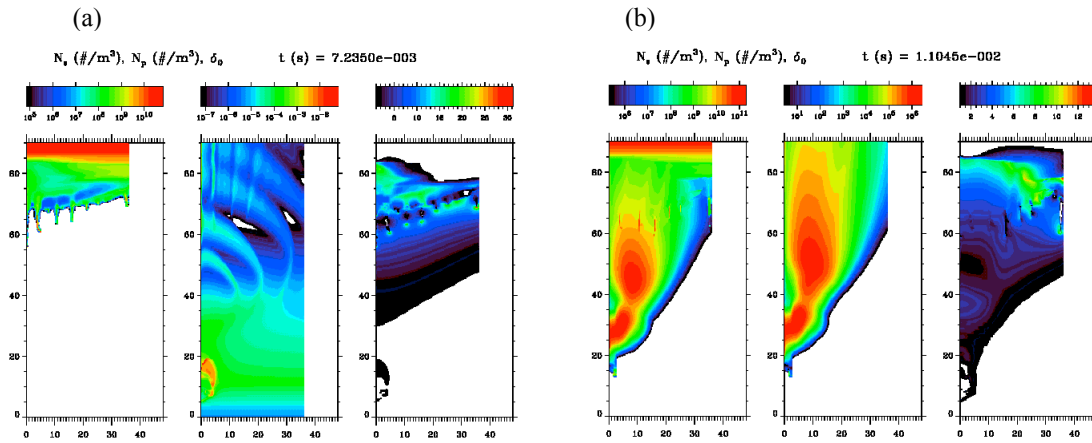
$$\begin{aligned}
\frac{\partial n_p}{\partial t} &= \nabla \cdot n_p \mathbf{v}_p + R_p n_p + F_c / \Delta_{\text{diff}} \\
\frac{\partial \mathbf{S}}{\partial t} &= \nabla \cdot \mathbf{S} \mathbf{v}_p - e n_p (\mathbf{E} + \mathbf{v}_p \times \mathbf{B}) \times \mathbf{S} \quad \text{where, } \mathbf{S} = \Delta n_p \mathbf{v}_p \\
\frac{\partial n_s}{\partial t} &= \nabla \cdot n_s \mathbf{v}_s + R_s n_p - \Delta n_s + \Delta_i n_s - \Delta_R n_+ n_s \\
\frac{\partial n_-}{\partial t} &= \nabla \cdot n_- \mathbf{v}_- + \Delta n_s - \Delta_I n_+ n_- \\
\frac{\partial n_+}{\partial t} &= \nabla \cdot n_+ \mathbf{v}_+ + R_s n_p + R_p n_p + \Delta_i n_s - \Delta_I n_+ n_- - \Delta_R n_+ n_s
\end{aligned} \tag{4}$$

SIMULATION RESULTS

In our model a high-altitude discharge/sprite is initiated by first producing a simulated positive cloud-to-ground discharge. We accomplish the latter by introducing negative charge into the cloud over a distributed spatial volume and within a certain period of time. In the simulation presented here we deposited 200 C at an altitude of 8 km over an ellipsoid with a maximum radial diameter of 6 km and a maximum thickness of 1 km. The time to build up the charge was set to 8 ms. The computational grid included 120 radial cells from 0–36 km and 300 vertical cells extending from 0-90 km altitude. The spatial resolution was 300 x 300 m. The ambient atmospheric conductivity was taken from the measurements of Hale [7].

After approximately 0.5 ms the electric field begins to exceed the threshold for runaway breakdown at an altitude of 83 km. This over-voltage (defined to be the ratio of the electric field to the threshold field necessary to initiate a runaway avalanche) grows in spatial extent and in magnitude as time proceeds. At 1.6 ms the threshold for conventional breakdown is exceeded over a region 4 km thick and 30 km in diameter. Conventional breakdown develops in this region and leads to an enhanced secondary electron population. The over-voltage continues to grow (to a value, $\Delta_b = 20$) until sufficient conductivity develops to eliminate the electric field over a sizeable region (2 km thick by 20 km in diameter). As the field increases an over-volted front develops below the field-depleted region and moves downward. In this region the ionization rate is slower than the electrical relaxation rate so that the field is eliminated rapidly behind the front as it moves downward with a speed $V_f \sim 5 \times 10^6$ m/s. At an altitude of 70 km the ionization rate exceeds the relaxation rate and charge builds up more rapidly than the field can be eliminated. In addition, the ionization rate is sufficiently high so as to cause a rapid increase in electron density. As a result inductive processes begin to contribute to further enhancement of the electric field and to the development of a streamer. The streamer itself increases the field around it and causes the development of another streamer that in turn contributes to initiation of other streamers and so on until approximately seven streamers are produced by 8 ms into the simulation. The streamers propagate at approximately $V_{st} \sim 8 \times 10^6$ m/s and terminate at an altitude of about 55 km where the ambient over-voltage is too weak to support further evolution of the streamer. It is also possible that our limited grid resolution does not permit sufficient field enhancement in front of the streamer head. A snapshot at ~ 7.2 ms into the simulation is provided in Fig. 1a and shows the spatial distribution of the secondary electron density (panel 1), the primary electron density (panel 2), and the over-voltage (panel 3).

A second process begins at approximately 10-11 ms into the simulation at which point the field is over-volted over a large altitude range from 15 km to 85 km altitude. At this stage a runaway discharge develops near the cloud top and is observed to propagate out of the top of the grid. Roughly 0.5 C of primary electrons exit the grid and a patch of secondary electrons forms at 45 km with a density of 10^{12} el m⁻³ and persists for several ms. A snapshot at ~ 11 ms into the simulation is provided in Fig. 1b in the same format as Fig. 1a.



Figs. 1(a) and 1(b). Simulation results for the secondary and primary electron densities (m^{-3}) and the over-voltage as a function of height (km) and radius (km) at 7.3 ms and 11 ms respectively.

CONCLUSIONS

Our sprite simulations show the development of both conventional streamers and a runaway discharge. The streamers will produce significant optical emissions (tens to hundreds of kR) from 55 km to 70 km with a morphology reminiscent of columniform sprites. Observations however indicate that these sorts of sprites tend to form at somewhat higher altitudes from 75-85 km [8]. An alternative mechanism for their formation is provided in [9]. The runaway discharge in our simulation will produce more than enough X- and γ -radiation in the 30-300 keV range to account for the BATSE measurements. The electron density patch produced at 45 km altitude is consistent with the measurements of Rumi, [10], see also [11]. The flux of energetic electrons out of our grid is large and suggests that runaway discharges could be contributing to the population of the radiation belts provided that these events are frequent enough on a global scale and at the appropriate L-shells. Further work is needed to establish the driving mechanism for sprite formation and to assess the impact of high-altitude discharges on the various chemical and electrical processes inherent to the mesosphere, ionosphere, and magnetosphere.

REFERENCES

- [1] C.J. Rodger, "Red sprites, upward lightning, and VLF perturbations," *Revs. of Geophys.*, vol. 37, 317-336, 1999.
- [2] C.T.R. Wilson, "The electric field of a thundercloud and some of its effects," *Proc. R. Soc. London*, vol. 37, 32D, 1925.
- [3] R.A. Armstrong, D.M. Suszcynsky, W.A. Lyons, T.E. Nelson, "Multi-color photometric measurements of ionization and energies in sprites," *GRL*, vol. 27, 653-656, 2000.
- [4] A.V. Gurevich, G.M. Milikh, and R.A. Roussel-Dupré, "Runaway electron mechanism of air breakdown and preconditioning during a thunderstorm," *Phys. Lett. A*, vol. 165, 463, 1992.
- [5] G.J. Fishman, P.N. Bhat, R. Mallozzi, J.M. Horack, T. Koshut, C. Kouveliotou, G.N. Pendleton, C.A. Meegan, R.B. Wilson, W.S. Paciesas, S.J. Goodman, H.J. Christian, "Discovery of intense gamma-ray flashes of atmospheric origin," *Science*, vol. 264, 1313, 1994.
- [6] R. Roussel-Dupre, E.M.D. Symbalisty, Y. Taranenko, V. Yukhimuk "Simulations of high-altitude discharges initiated by runaway breakdown," *JASTP*, vol. 60, 917-940, 1998.
- [7] L.C. Hale, C.L. Croskey, and J.D. Mitchell, "Measurements of middle-atmosphere electric fields and associated electrical conductivities," *GRL*, vol 8, 928-930, 1981.
- [8] E.M. Wescott, D.D. Sentman, M.J. Heavner, D.L. Hampton, W.A. Lyons, and T. Nelson, "Observations of columniform sprites," *JASTP*, vol. 60, 733-740, 1998.
- [9] E.M.D. Symbalisty, R.A. Roussel-Dupre, D.O. Revelle, D.M. Suszcynsky, V.A. Yukhimuk, and M.J. Taylor, "Meteor Trails and Columniform Sprites," *Icarus*, vol. 148, 65-79, 2000.
- [10] G.C. Rumi, "VHF radar echoes associated with atmospheric phenomena," *JGR*, vol. 62, 547-564, 1957.
- [11] R. Roussel-Dupre and E. Blanc, "HF Echoes from ionization potentially produced by high-altitude discharges," *JGR*, vol. 102, 4613-4622, 1997.